

## Nuclear $\gamma$ rays from 720-MeV $\alpha$ -induced reactions on $^{27}\text{Al}$ and $^{28}\text{Si}$

B. J. Lieb

*George Mason University, Fairfax, Virginia 22030*

H. S. Plendl

*Florida State University, Tallahassee, Florida 32306*

H. O. Funsten

*College of William and Mary, Williamsburg, Virginia 23186*

C. E. Stronach

*Virginia State University, Petersburg, Virginia 23803*

V. G. Lind

*Utah State University, Logan, Utah 84322*

(Received 7 February 1980)

Prompt  $\gamma$  rays from the interaction of 720-MeV  $\alpha$  particles with  $^{27}\text{Al}$  and  $^{28}\text{Si}$  were detected and analyzed to identify residual nuclei and to determine cross sections for production of specific levels. No  $\gamma$ -ray transitions were detected from nuclei heavier than the target. From Doppler broadening, the momentum of the residual nuclei was estimated. The results are compared with previous results for 140- and 1600-MeV  $\alpha$ 's on  $^{27}\text{Al}$  and  $\sim 200$ -MeV  $\pi^+$  on  $^{27}\text{Al}$  and  $^{28}\text{Si}$  and fitted to a spallation-yield formula.

[NUCLEAR REACTIONS  $^{27}\text{Al}(\alpha, X\gamma)$ ,  $^{28}\text{Si}(\alpha, X\gamma)$ ,  $E_\alpha = 720$  MeV; detected  $\gamma$  rays, Ge(Li); measured  $E_\gamma$ ,  $90^\circ\sigma$  for specific levels in residual nuclei, Doppler broadening for recoil momentum.]

### I. INTRODUCTION

We have studied  $\gamma$  rays from the inclusive reactions of 720-MeV (180 MeV/nucleon)  $\alpha$  particles on the odd- $Z$ , even- $N$  nucleus  $^{27}\text{Al}$  and its even- $Z$ , even- $N$  neighbor  $^{28}\text{Si}$  in order to complement earlier studies of these nuclei with  $\pi^+$  at the  $\Delta(1232)$  resonance.<sup>1,2</sup> Although alphas and pions have quite different properties, several factors suggest that the gross features of their interactions may be similar. The opacity of nuclear matter to  $\pi^+$ 's near the  $\Delta(1232)$  resonance and to energetic  $\alpha$ 's is of the same magnitude. Peripheral interactions may, therefore, be of similar importance for both of these probes. Furthermore, the interaction range of  $\pi$ - $N$  is also comparable to that of  $\alpha$ - $N$ . Simultaneous reactions with several nucleons, either correlated or uncorrelated, should, therefore, be nearly equally likely. In addition, both particles are bosons with spin zero.

Two inherently different properties of pions are that they can form resonances with target nucleons and that their mass energy can be transformed into nuclear excitation energy. An additional difference between the alphas and pions used in our experiments is their kinetic energy ( $E_\alpha = 720$  MeV,  $E_\pi = 200$  MeV) and hence their velocity ( $\beta_\alpha = 0.55$ ,

$\beta_\pi = 0.9$ ) and wavelength. The kinetic energy per nucleon in the incident  $\alpha$ , 180 MeV, is, however, close to that of the pions. The similarities are likely to govern the gross features of the interaction, while the unique properties of the particles and their reaction mechanisms should show up in specific reaction channels.

The present experiment, which studied the interaction of  $\alpha$ 's with  $^{27}\text{Al}$  and  $^{28}\text{Si}$  at  $E_\alpha = 720$  MeV by detecting prompt  $\gamma$  rays from residual nuclei, complements several other  $\alpha$  experiments. In an earlier comprehensive experiment, prompt  $\gamma$  rays<sup>3</sup> and mass fragments<sup>4</sup> from interactions of 140-MeV  $\alpha$ 's on  $^{27}\text{Al}$  have been detected. Prompt  $\gamma$  rays resulting from 1.6-GeV  $\alpha$ 's (and also from 3 and 4.8 GeV  $^{12}\text{C}$  ions) on Na, S, and Ca have been detected in another study.<sup>5</sup> Mass fragments from 720-MeV  $\alpha$ 's on Al, Ag, and Ta have been detected in an extensive study<sup>6-8</sup> with the same beam that was used in the present work.

### II. EXPERIMENT AND DATA ANALYSIS

The experiment was performed at the Space Radiation Effects Laboratory (SREL) using the external 720-MeV  $\alpha$  beam from the synchrocyclotron. A stochastic "cee" was used to spread out

the internal beam in time; the prompt beam bursts were gated out electronically. The extracted beam spot size was  $\sim 3.5$  cm in diameter, and the intensity was  $6 \times 10^5$   $\alpha$ /sec.

Natural targets of 4.75 g/cm<sup>2</sup> Al and 5.03 g/cm<sup>2</sup> Si were oriented at an angle of 45° with respect to the beam. The  $\gamma$  rays were detected by a Ge(Li) detector of 11% efficiency in coincidence with an incident  $\alpha$ -particle signature in a two-scintillator beam telescope and in anticoincidence with signals from a cup-shaped scintillator which surrounded the Ge(Li) detector to eliminate charged-particle events. The Ge(Li) detector was located at 90° with respect to the beam direction. Gamma rays from 0.25 to 5.5 MeV were recorded in a gain-stabilized 2048-channel analyzer with a resolution of  $\sim 2.7$  keV. Portions of the  $\gamma$ -ray spectra from the Al and Si targets were compared in Fig. 1.

In analyzing the  $\gamma$ -ray spectra, an attempt was made to locate  $\gamma$  transitions from the seven or eight lowest excited states of every possible residual nucleus using information contained in the compilations of Ajzenberg-Selove<sup>9</sup> and Endt and Van der Leun.<sup>10</sup> In addition, a search was made

for the higher energy states that were observed in the experiment with 140-MeV  $\alpha$ 's on <sup>27</sup>Al.<sup>3</sup> Cross sections were computed from the target parameters, the integrated beam flux, and the peak areas as determined by fitting them to a Gaussian with an exponential background. In this calculation, it was assumed that  $\gamma$  rays were emitted isotropically. Major contributions to the reported uncertainties were statistics, the energy-dependent error in the relative efficiency, and the error in absolute efficiency normalization, which was estimated to be 15%.

### III. RESULTS AND DISCUSSION

#### A. General features of the residual mass spectra

The measured cross sections for 720-MeV  $\alpha$ 's on <sup>27</sup>Al and <sup>28</sup>Si (Table I) are reported in two ways:  $\sigma_{\text{tot}}$  is the total cross section for production of a particular state, either by direct excitation or by feeding from higher states;  $\sigma_{\text{ex}}$  is  $\sigma_{\text{tot}}$  corrected for feeding from identified higher states. Transitions were observed corresponding to excitation of states in the target nucleus, but these are not reported due to probable contamination from secondary ( $n, n'$ ) scattering. It should be noted, however, that the yield of  $\gamma$  rays from <sup>27</sup>Al at 720 MeV is equal, within uncertainties, to the measured yield at 140 MeV from a thin target for which the ( $n, n'$ ) scattering contribution is negligible.<sup>3</sup> In the <sup>28</sup>Si spectrum,  $\gamma$  decays from states of <sup>29</sup>Si and <sup>30</sup>Si were detected. The observed cross sections for these states support the assumption that they are due to ( $\alpha, \alpha'$ ) and secondary ( $n, n'$ ) scattering on the <sup>29</sup>Si and <sup>30</sup>Si nuclei (which have abundances of  $\sim 5\%$  and  $\sim 3\%$ , respectively) in the natural Si target. The cross section for production of the 4.439 MeV state of <sup>12</sup>C should be considered uncertain because of possible  $\alpha$  interactions within the <sup>12</sup>C scintillation counters.

The sum of all measured cross sections is 390 mb for each target. This is about  $\frac{1}{3}$  of the geometrical cross section. It becomes systematically more difficult to detect  $\gamma$  rays from the residual nuclei with  $A \lesssim 18$ .  $\gamma$  rays emitted by these lighter nuclei show a more pronounced Doppler broadening, making transitions from weakly excited states more difficult to detect. Because of the generally short lifetime of radioactive isotopes in this mass region, use of the off-beam radioactivity studies would not appreciably increase the available data.

The average number of protons and neutrons removed in these reactions is similar ( $\Delta Z \approx 2.2$ ,  $\Delta N \approx 2.3$  for <sup>27</sup>Al, and  $\Delta Z \approx 2.6$ ,  $\Delta N \approx 2.1$  for <sup>28</sup>Si), but a detailed comparison of individual cross sections reveals differences. In order to eliminate

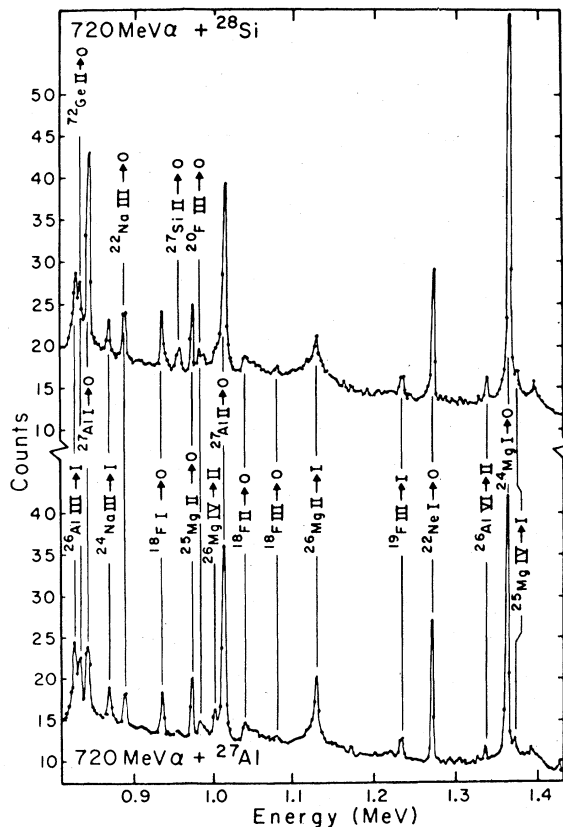


FIG. 1. Portions of the experimental  $\gamma$ -ray spectra for 720-MeV  $\alpha$  particles on <sup>27</sup>Al and <sup>28</sup>Si.

TABLE I. Measured cross sections for production of residual nuclei from  $^{27}\text{Al}$  and  $^{28}\text{Si}$  at  $E_\alpha = 720$  MeV.

Residual nucleus	$E$ (MeV)	$J^\pi$	$\alpha + ^{27}\text{Al}$		$\alpha + ^{28}\text{Si}$	
			$\sigma_{\text{tot}}(\text{mb})^a$	$\sigma_{\text{ex}}(\text{mb})^b$	$\sigma_{\text{tot}}(\text{mb})^a$	$\sigma_{\text{ex}}(\text{mb})^b$
$^{27}\text{Si}$	0.780	$\frac{1}{2}^+$			$9.2 \pm 1.6$	$8.7 \pm 1.6$
	0.957	$\frac{3}{2}^+$			$8.7 \pm 1.5$	$8.7 \pm 1.5$
	2.164	$\frac{7}{2}^+$			$1.9 \pm 0.4$	$1.9 \pm 0.4$
$^{27}\text{Al}$	0.844	$\frac{1}{2}^+$			$24 \pm 5^c$	$23 \pm 5^c$
	1.014	$\frac{3}{2}^+$			$29 \pm 5^c$	$29 \pm 5^c$
	2.211	$\frac{7}{2}^+$			$13 \pm 2^c$	$11 \pm 2^c$
	3.004	$\frac{9}{2}^+$			$14 \pm 3^c$	$14 \pm 2.9^c$
$^{26}\text{Al}$	0.417	$3^+$	$19 \pm 4$	$15 \pm 4$	$21 \pm 5$	$17 \pm 5$
	1.058	$1^+$	$10 \pm 2$	$10 \pm 2$	$10 \pm 3$	$10 \pm 3$
	1.759	$2^+$	$1.8 \pm 0.3$	$1.8 \pm 0.3$	$2.5 \pm 0.5$	$2.5 \pm 0.5$
	2.069	$4^+$	$3.1 \pm 0.7$	$3.1 \pm 0.7$	$2.0 \pm 0.6$	$1.0 \pm 0.7$
	2.365	$3^+$	d	d	$1.9 \pm 0.6$	$1.9 \pm 0.6$
$^{26}\text{Mg}$	1.809	$2^+$	$75 \pm 13$	$50 \pm 10$	$19 \pm 3$	$6.1 \pm 4.0$
	2.938	$2^+$	$25 \pm 5$	$21 \pm 4$	$12 \pm 3$	$8.7 \pm 3.1$
	3.588	$0^+$	$1.5 \pm 0.4$	$1.5 \pm 0.4$	d	d
	3.940	$3^+$	$6.0 \pm 1.5$	$6.0 \pm 1.5$	$5.4 \pm 1.0$	$5.4 \pm 1.0$
$^{25}\text{Al}$	0.452	$\frac{1}{2}^+$	$4.2 \pm 0.9^e$	$3.6 \pm 0.9^e$	$9.3 \pm 2.1^e$	$8.2 \pm 2^e$
	0.945	$\frac{3}{2}^+$	$1.1 \pm 0.3$	$1.1 \pm 0.3$	$2.0 \pm 0.5$	$2.0 \pm 0.5$
$^{25}\text{Mg}$	0.585	$\frac{1}{2}^+$	$17 \pm 3$	$7.2 \pm 2.6$	$16 \pm 3$	$9.4 \pm 3.1$
	0.975	$\frac{3}{2}^+$	$14 \pm 3$	$13 \pm 3$	$12 \pm 2$	$11 \pm 2$
	1.965	$\frac{5}{2}^+$	$5.5 \pm 1.1$	$5.5 \pm 1.1$	$2.2 \pm 0.6$	$2.2 \pm 0.6$
$^{24}\text{Mg}$	1.369	$2^+$	$58 \pm 9$	$40 \pm 8$	$63 \pm 10$	$55 \pm 10$
	4.123	$4^+$	$18 \pm 4$	$18 \pm 4$	$7.1 \pm 2.8$	$7.1 \pm 2.8$
	4.238	$2^+$	d	d	$0.4 \pm 0.1$	$0.4 \pm 0.1$
	5.236	$3^+$	$0.6 \pm 0.2$	$0.6 \pm 0.2$	$0.2 \pm 0.1$	$0.2 \pm 0.1$
$^{23}\text{Na}$	0.440	$\frac{5}{2}^+$	$34 \pm 8$	$34 \pm 8$	$26 \pm 6$	$26 \pm 6$
	2.391	$\frac{1}{2}^+$	$<1.0$	$<1.0$	$1.0 \pm 0.3$	$1.0 \pm 0.3$
$^{22}\text{Mg}$	1.246	$2^+$	$<0.8$	$<0.8$	$0.9 \pm 0.2$	$0.9 \pm 0.2$
$^{22}\text{Na}$	0.891	$4^+$	$5.4 \pm 1.0$	$5.2 \pm 1.0$	$6.0 \pm 1.1$	$5.8 \pm 1.1$
	1.528	$5^+$	$5.3 \pm 1.0$	$5.3 \pm 1.0$	$5.0 \pm 1.1$	$5.0 \pm 1.1$
	1.984	$3^+$	$1.9 \pm 0.6$	$1.9 \pm 0.6$	$2.0 \pm 0.4$	$2.0 \pm 0.4$
	2.211	$1^-$	$0.8 \pm 0.2$	$0.8 \pm 0.2$	$1.0 \pm 0.2$	$1.0 \pm 0.2$
	2.571	$2^-$	$0.9 \pm 0.2$	$0.9 \pm 0.2$	$1.0 \pm 0.2$	$1.0 \pm 0.2$
$^{22}\text{Ne}$	1.275	$2^+$	$26 \pm 4$	$24 \pm 4$	$14 \pm 3$	$13 \pm 3$
	3.357	$4^+$	$1.5 \pm 0.2$	$1.5 \pm 0.2$	$1.0 \pm 0.4$	$1.0 \pm 0.4$
$^{21}\text{Na}$	0.332	$\frac{5}{2}^+$	$1.8 \pm 0.5$	$1.8 \pm 0.5$	$2.8 \pm 0.8$	$2.8 \pm 0.8$
	2.425	$\frac{1}{2}^+$	d	d	$0.6 \pm 0.2$	$0.6 \pm 0.2$
$^{21}\text{Ne}$	0.351	$\frac{5}{2}^+$	$28 \pm 7$	$27 \pm 7$	$19 \pm 5$	$18 \pm 5$
	2.788	$\frac{1}{2}^-$	$0.9 \pm 0.3$	$0.9 \pm 0.3$	$0.7 \pm 0.2$	$0.7 \pm 0.2$

TABLE I. (Continued)

Residual nucleus	$E$ (MeV)	$J^\pi$	$\alpha + {}^{27}\text{Al}$		$\alpha + {}^{28}\text{Si}$	
			$\sigma_{\text{tot}}$ (mb) <sup>a</sup>	$\sigma_{\text{ex}}$ (mb) <sup>b</sup>	$\sigma_{\text{tot}}$ (mb) <sup>a</sup>	$\sigma_{\text{ex}}$ (mb) <sup>b</sup>
${}^{21}\text{F}$	0.280	$\frac{1}{2}^+$	<0.4	<0.4	<0.5	<0.5
${}^{20}\text{Ne}$	1.634	$2^+$	$17 \pm 3$	$13 \pm 3$	$17 \pm 3$	$13 \pm 3$
	4.968	$2^-$	$3.6 \pm 0.8$	$3.6 \pm 0.8$	$3.7 \pm 0.8$	$3.7 \pm 0.8$
${}^{20}\text{F}$	0.656	$3^+$	$4.0 \pm 0.8$	$4.0 \pm 0.8$	$1.8 \pm 0.4$	$1.7 \pm 0.4$
	0.984	$1^-$	d	d	$1.7 \pm 0.6$	$1.7 \pm 0.6$
	1.309	$2^-$	$1.2 \pm 0.4$	$1.2 \pm 0.4$	$0.6 \pm 0.3$	$0.6 \pm 0.3$
${}^{20}\text{O}$	1.674	$2^+$	<0.7	<0.7	<0.9	<0.9
${}^{19}\text{Ne}$	0.238	$\frac{5}{2}^+$	$1.2 \pm 0.4$	$1.2 \pm 0.4$	$1.5 \pm 0.5$	$1.5 \pm 0.5$
	0.275	$\frac{1}{2}^-$	$1.3 \pm 0.4$	$1.3 \pm 0.4$	$1.7 \pm 0.5$	$1.7 \pm 0.5$
${}^{19}\text{F}$	1.346	$\frac{5}{2}^-$	$6.0 \pm 1.1$	$6.0 \pm 1.1$	$4.7 \pm 1.3$	$4.7 \pm 1.3$
	2.780	$\frac{9}{2}^+$	$1.4 \pm 0.3$	$1.4 \pm 0.3$	$0.9 \pm 0.2$	$0.9 \pm 0.2$
${}^{18}\text{Ne}$	1.887	$2^+$	<0.8	<0.8	<0.6	<0.6
${}^{18}\text{F}$	0.937	$3^+$	$5.1 \pm 0.9$	$5.1 \pm 0.9$	$5.8 \pm 1.0$	$5.8 \pm 1.0$
	1.042	$0^+$	$4.0 \pm 1.7$	$4.0 \pm 1.7$	$3.4 \pm 1.5$	$3.4 \pm 1.5$
	1.081	$0^-$	$0.6 \pm 0.3$	$0.6 \pm 0.3$	$1.0 \pm 0.3$	$1.0 \pm 0.3$
${}^{18}\text{O}$	1.982	$2^+$	$6.1 \pm 1.3$	$3.9 \pm 1.2$	$3.1 \pm 0.6$	$2.1 \pm 0.6$
	3.555	$4^+$	$2.2 \pm 0.4$	$2.2 \pm 0.4$	$1.0 \pm 0.2$	$1.0 \pm 0.2$
${}^{17}\text{O}$	0.871	$\frac{1}{2}^+$	$5.0 \pm 1.0$	$5.0 \pm 1.0$	$3.3 \pm 0.6$	$3.3 \pm 0.6$
${}^{16}\text{O}$	6.130	$3^-$	$8.1 \pm 2.3$	$8.1 \pm 2.3$	$10 \pm 3$	$10 \pm 3$
${}^{15}\text{O}$	5.241	$\frac{5}{2}^+$	$1.0 \pm 0.3$	$1.0 \pm 0.3$	$1.0 \pm 0.3$	$1.0 \pm 0.3$
${}^{15}\text{N}$	5.270	$\frac{5}{2}^+$	$3.4 \pm 1.0$	$3.4 \pm 1.0$	$2.9 \pm 0.8$	$2.9 \pm 0.8$
${}^{15}\text{C}$	0.740	$\frac{5}{2}^+$	<1.1	<1.1	<0.4	<0.4
${}^{13}\text{C}$	3.854	$\frac{5}{2}^+$	$4.1 \pm 1.0$	$4.1 \pm 1.0$	$2.4 \pm 0.6$	$2.4 \pm 0.6$
${}^{12}\text{C}$	4.439	$2^+$	$11 \pm 3^f$	$11 \pm 3^f$	$8.5 \pm 2.0^f$	$8.5 \pm 2.0^f$
${}^{10}\text{B}$	0.718	$1^+$	$6.3 \pm 1.1^f$	$6.3 \pm 1.1^f$	$5.9 \pm 1.1^f$	$5.9 \pm 1.1^f$

<sup>a</sup>  $\sigma_{\text{tot}}$  is the cross section for production of the state, including  $\gamma$ -ray feeding from high states.

<sup>b</sup>  $\sigma_{\text{ex}}$  is  $\sigma_{\text{tot}}$  corrected for  $\gamma$ -ray feeding from higher states known to be excited.

<sup>c</sup> Cross sections for  ${}^{27}\text{Al}$  may contain contributions from  $(n, n')$  reactions in the Al casing of the Ge(Li) detector.

<sup>d</sup> Cross section could not be determined.

<sup>e</sup> Cross sections should be considered as upper limits because of overlap with the  ${}^{23}\text{Mg}$  0.451 MeV transition.

<sup>f</sup> Cross sections for  ${}^{12}\text{C}$  and  ${}^{10}\text{B}$  should be considered as upper limits because of possible contamination from  $\alpha$  reactions in the scintillators.

the effects of  $\gamma$ -decay systematics on these cross sections, we will present ratios of the summed cross sections ( $\sum_i \sigma_{\text{ex}, i}$ ) for a given residual nucleus, for different incident projectiles and targets. Table II shows the summed cross-section ratios  $\sigma(\alpha + {}^{28}\text{Si})/\sigma(\alpha + {}^{27}\text{Al})$ . Ratios whose uncertainties exceed 40% have been excluded from this and later

tables, but most errors are less than 20%. The ratios are seen to be  $<1$  on the  $N > Z$  side of the valley of stability and  $>1$  on the  $N < Z$  side. Thus the initial condition that  $Z/N < 1$  for the  ${}^{27}\text{Al}$  target persists and produces a cross-section distribution shifted towards  $N > Z$  for that nucleus. It is unlikely that a reaction mechanism in which evapora-

TABLE II. Cross section ratios for production of residual nuclei,  $\sigma(^{28}\text{Si})/\sigma(^{27}\text{Al})$  at  $E_\alpha = 720$  MeV, based on data from Table I.

$N \backslash Z$	5	6	7	8	9	10	11	12	13	14
13 (Al)								2.2	1.1	
12 (Mg)								1.1	0.88	0.26
11 (Na)						1.9	1.0	0.79		
10 (Ne)					1.3	1.0	0.67	0.55		
9 (F)					1.1	0.76	0.77			
8 (O)			1.0	1.2	0.66	0.51				
7 (N)				0.85						
6 (C)		0.77	0.59							
5 (B)	0.94									

tion is the only means of nucleon removal would produce such an asymmetry in the cross-section ratios.

#### B. Production of residual nuclei heavier than the target nucleus

There is no evidence in our results for formation of residual nuclei heavier than the target nucleus for either target. Glascock *et al.*<sup>3</sup> found in their experiment with 140 MeV  $\alpha$ 's on  $^{27}\text{Al}$  that ~8% of the total cross section was for  $A > 27$  residual nuclei. But Shibata *et al.*<sup>5</sup> in their work with 1.6 GeV  $\alpha$ 's on Na, S, and Ca found no  $\gamma$ -ray transitions from residual nuclei heavier than the target. They conclude that nucleon transfer in the high-energy region falls off with increasing projectile velocity according to the momentum mismatch of the nucleon in the nucleus. Thus for beam energies above the Fermi energy of 50 MeV/ $N$ , such transfer should become small. It is, of course, possible that nucleons are transferred to the target but that such transfer results primarily in highly excited states which decay by particle emission to nuclei with  $A$  less than the target.

#### C. Doppler broadening and recoil momentum of the residual nucleus

The Doppler broadening of spectral lines makes it possible to compute the momentum of the residual nucleus,  $\Delta p$ . At the same time it may obscure some weakly excited lines that feed lower-energy, relatively long-lived transitions which could otherwise be detected. In the present work, only a few  $\gamma$  transitions were found to be significantly Doppler broadened (Table III). The recoil momentum  $\Delta p$  was computed from the width of the Doppler-broadened line shape using the method of Lewis.<sup>11</sup> The uncertainty in these results is ~30%. The calculated  $\Delta p$ 's vary widely around an average value of ~190 MeV/ $c$ , which is of the same order as the nucleon Fermi momentum.

In the results<sup>3</sup> at  $E_\alpha = 140$  MeV, a larger number of Doppler-broadened lines were reported, and the broadening of these lines was generally greater than what we observed. In the results<sup>5</sup> at  $E_\alpha = 1.6$  GeV the average  $\Delta p$  was found to be ~200 MeV/ $c$ , similar to our results. Although no residual states with half-lives shorter than 250 fs were observed in the work at 1.6 GeV, the authors conclude that they are probably not missing

TABLE III. Doppler-broadened line widths of short-lived states in residual nuclei produced at  $E_\alpha = 720$  MeV.

Residual nucleus	$E_{\text{ex}}$ (MeV)	$\tau_m$ (fs)	$\alpha + ^{27}\text{Al}$		$\alpha + ^{28}\text{Si}$	
			FWHM (keV)	$\Delta p$ (MeV/ $c$ )	FWHM (keV)	$\Delta p$ (MeV/ $c$ )
$^{27}\text{Si}$	2.164	50			18	140
$^{27}\text{Al}$	2.211	39			24	180
	3.004	88			47	270
$^{26}\text{Mg}$	2.938	200	6.0	210	12	220
	3.941	900	6.9	200	7.2	150
$^{24}\text{Mg}$	4.123	55	41	230	40	220
$^{12}\text{C}$	4.439	61	91	140	70	110



TABLE V. Cross section ratios for production of residual nuclei,  $\sigma(\alpha_{720} + {}^{28}\text{Si})/\sigma(\pi_{200}^- + {}^{28}\text{Si})$ , based on data from Table I and Ref. 1.

$N \backslash Z$	5	6	7	8	9	10	11	12	13	14
14 (Si)									1.4	
13 (Al)								0.77	1.3	3.1
12 (Mg)								2.3	1.5	1.2
11 (Na)						1.8	2.2	1.2		
10 (Ne)					1.5	1.5	0.91	1.5		
9 (F)					3.4	1.9				
8 (O)				2.2	1.8	1.6				
7 (N)				2.2						
6 (C)		1.2								
5 (B)	1.0									

most convincing evidence, however, the excitation of certain specific higher-energy states of residual nuclei, is not observed in our work, possibly because these states are obscured by Doppler broadening.

E. Comparison of 720-MeV  $\alpha$ -induced reaction cross sections with 200-MeV  $\pi^+$ -induced reaction cross sections on  ${}^{27}\text{Al}$  and  ${}^{28}\text{Si}$

The reactions of  $\sim 200$ -MeV  $\pi^+$  on  ${}^{27}\text{Al}$  and  ${}^{28}\text{Si}$  have been studied previously by our group.<sup>1</sup> Since the opacity of the  $\pi$  at the  $\Delta(1232)$  resonance is similar that that of the  $\alpha$ , it might be expected that the cross sections for multinucleon removal would be similar, especially if the process is mainly evaporative.

In Table V, the ratio of the present 720-MeV  $\alpha$  cross sections to our earlier 200-MeV  $\pi^-$  cross sections<sup>1</sup> on  ${}^{28}\text{Si}$  is shown. Since the total measured cross section was 390 mb for  $\alpha$  and 240 mb for  $\pi^-$ , an average ratio should be 1.6. While there is no clear trend in ratios shown in Table V, a few general observations can be made. The pions, despite their lower energy, are more effective in removing large numbers of nucleons,  $\Delta A \geq 18$ , probably because the pion mass can be absorbed as excitation energy. The role of  $\pi$  absorption is clarified by Table VI, which compares relative cross sections for production of residual nuclei from reactions on  ${}^{27}\text{Al}$  induced by  $\alpha$ 's and  $\pi^+$ 's when only the residual  $\gamma$ 's were detected and by  $\pi^+$ 's when the residual  $\gamma$ 's were detected in coincidence with outgoing  $\pi^+$ 's at  $35^\circ$ .<sup>2</sup> In the latter, the requirements of an outgoing  $\pi$  coincidence eliminates absorption reactions. As expected, these coincidence cross sections are smaller for large  $\Delta A$  than the  $\alpha$  or  $\pi^-$  singles cross sections.

Shibata *et al.*<sup>5</sup> plotted cross sections for produc-

tion of even-even  $N=Z$  residual nuclei by  $\pi^-$ ,  $p$ ,  $\alpha$ , and  ${}^{12}\text{C}$  reactions on  ${}^{40}\text{Ca}$ . They found that while the  $\pi^-$  cross sections fell off exponentially with increasing  $\Delta A$ , the proton cross sections showed a small plateau and the  $\alpha$  and  ${}^{12}\text{C}$  cross sections showed a more definite plateau. They conclude that the exponential falloff of the  $\pi$  cross sections is due to the mainly statistical evaporation from intermediate excited states of  ${}^{40}\text{Ca}$  or its neighbors, and that the plateau observed for  ${}^{12}\text{C}$  and  $\alpha$  cross sections indicates a greater range of intermediate excited states following the cascade.

Figures 2 and 3 indicate an exponential falloff of the cross sections for the first excited  $2^+$  states (second excited  $3^-$  state of  ${}^{16}\text{O}$ ) of self-conjugate residual nuclei in our  $\alpha$  and  $\pi^+$  reactions on  ${}^{27}\text{Al}$  and  ${}^{28}\text{Si}$ . (The points for  ${}^{12}\text{C}$  production are not plotted because of possible contamination from reactions in the scintillator and possible double counting; those points would, in each case, fall

TABLE VI. Relative cross sections for production of residual nuclei from reactions on  ${}^{27}\text{Al}$  by alphas and pions (see text). The cross sections are normalized to 1 for the  ${}^{26}\text{Mg } I \rightarrow 0$  transition.

Transition	$\sigma(\alpha)^a$	$\sigma(\pi^+ \text{ singles})^b$	$d\sigma/d\Omega(35^\circ\pi^-)^c$
${}^{26}\text{Al } (II \rightarrow 0)$	0.25	0.23	0.17
${}^{26}\text{Mg } (I \rightarrow 0)$	1.0	1.0	1.0
${}^{26}\text{Mg } (II \rightarrow 0)$	0.33	0.26	0.28
${}^{25}\text{Mg } (I \rightarrow 0)$	0.23	0.14	0.10
${}^{24}\text{Mg } (I \rightarrow 0)$	0.77	0.76	0.52
${}^{23}\text{Na } (I \rightarrow 0)$	0.45	0.47	0.15
${}^{21}\text{Ne } (I \rightarrow 0)$	0.37	0.30	0.07 <sup>d</sup>

<sup>a</sup> Present work.

<sup>b</sup> Reference 12.

<sup>c</sup> Reference 2.

<sup>d</sup> May be low because of electronics discriminator cut-off.

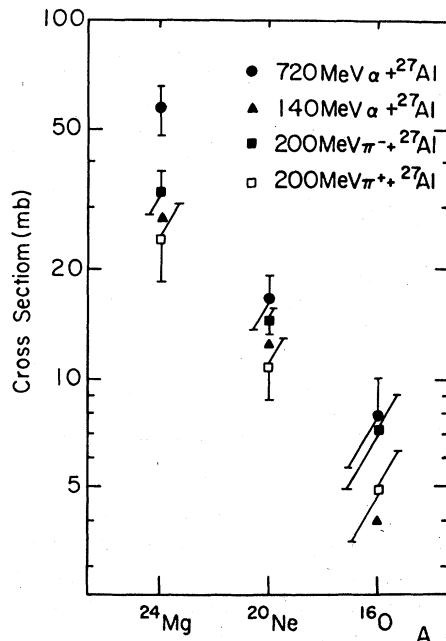


FIG. 2. Cross sections for production of self-conjugate residual nuclei from  $^{27}\text{Al}$  plotted as a function of decreasing  $A$  of the residual nucleus.

above the exponential line.) The 140-MeV  $\alpha + ^{27}\text{Al}$  results (Fig. 2) also show an exponential falloff. These results suggest that  $\alpha$ -induced reactions at 720 and 140 MeV on  $^{27}\text{Al}$ , as well as  $\pi^-$  induced

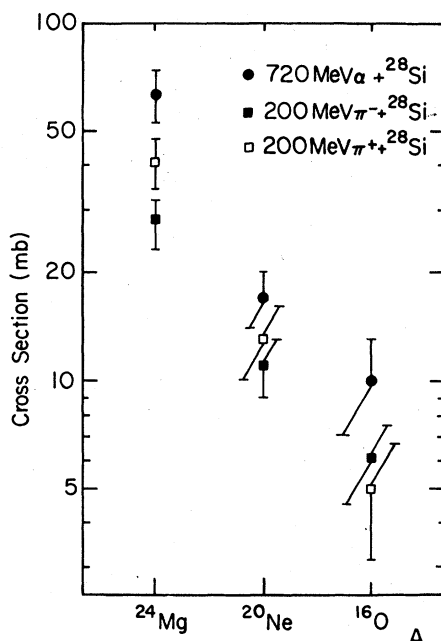


FIG. 3. Cross sections for production of self-conjugate residual nuclei from  $^{28}\text{Si}$  plotted as a function of decreasing  $A$  of the residual nucleus.

reactions at 200 MeV, result primarily in statistical evaporation.

#### F. Comparison of 720-MeV $\alpha$ -induced reaction cross sections with spallation yield calculations

Yields from spallation experiments have been successfully parametrized by several formulas developed by Rudstam.<sup>13</sup> In order to compare the present results with the Rudstam formulation which predicts the total yield for a particular residual nucleus, it is necessary to estimate the fraction of the production of each residual nucleus that is missed by the  $\gamma$ -ray technique. Unfortunately, the fraction of missed cross section will vary with the  $\gamma$ -decay schemes of each residual nucleus. In even-even nuclei, most transitions strongly feed the lowest  $2^+$  states, making it likely that a large fraction of the total cross section for an even-even nucleus is detected. Inspection of the  $\gamma$ -decay schemes of even-even nuclei in this mass region indicates that  $\sim 80\%$  of states for which the  $\gamma$ -decay branching ratios are known feed the first excited state, either directly or indirectly. The corresponding fraction for non-even-even nuclei averages  $\sim 30\%$  but ranges from 75% down to 15%.

Using a procedure discussed in detail in a previous paper,<sup>12</sup> we have compensated the present cross sections for the effects of variation in feeding. This compensation is performed by dividing the value of the measured  $i$ th state cross section (not corrected for feeding from higher energy states) by the fraction of the total production of that nucleus which decays through the  $i$ th state. In calculating this fraction, we used available  $\gamma$ -ray feeding information and assumed a statistical  $2J+1$  initial population of all states. The resultant compensated cross section ( $\sigma_c$ ), usually calculated for the lowest state detected, should then be equal to the total production cross section for that nucleus under the assumption of a statistical population of states.

Values of  $\sigma_c$  (except for production of  $^{12}\text{C}$  and  $^{10}\text{B}$  which may have background contributions) were then fitted to the Rudstam<sup>13</sup> formula:

$$\sigma(Z, A) = \sigma_0 \exp[-P(A_t - A) - RX^2],$$

where  $X \equiv Z - SA$  and  $Z$  and  $A$  refer to the residual nucleus;  $\sigma_0$ ,  $P$ ,  $R$ , and  $S$  are free parameters, and  $A_t$  is the  $A$  of the target. This formula corresponds to an exponential mass-yield distribution and a Gaussian charge distribution reflecting the valley of stability. The fitted parameters ( $P = 0.16, 0.13$ ;  $R = 4.0, 4.5$ ; and  $S = 0.490, 0.491$ , respectively, for  $^{27}\text{Al}$  and  $^{28}\text{Si}$ ) are in reasonable agreement with those of Rudstam.



Dividing  $\sigma_c$  by  $\sigma_0 \exp[-P(A_t - A)]$  removes the exponential behavior and allows the fit to be presented graphically. The resultant renormalized cross sections are compared with the function  $\exp(-RX^2)$  in Figs. 4 and 5. The error bars plotted are the quoted errors minus the error due to absolute normalization plus the estimated error in the compensation process. The latter estimate was made by assuming that the error was proportional to the magnitude of the compensation.

Values of  $\sigma_c$  clearly follow the trends in the spallation yields for both targets. This supports the assumption of the compensation process that the initial population of states is statistical. A major exception is the  $^{24}\text{Mg}$  cross section for the  $^{28}\text{Si}$  target. (The error in  $\sigma_c$  for  $^{22}\text{Na}$  is too large to attach any significance to that value.) The production of  $^{24}\text{Mg}$ , which is one  $\alpha$  particle removed from the even-even  $^{28}\text{Si}$  target, is larger than would be expected from a spallation process.

#### IV. SUMMARY AND CONCLUSIONS

Our results can be summarized as follows:

1. Prompt nuclear  $\gamma$  rays following 720-MeV  $\alpha$  reactions on  $^{27}\text{Al}$  and  $^{28}\text{Si}$  were detected from approximately twenty-five residual nuclei. The sum of the measured cross sections is  $\sim 380$  mb for each target, i. e.,  $\sim \frac{1}{3}$  of the geometrical cross

section.

2. There was not evidence for residual nuclei with  $A$  greater than the target.

3. Cross sections for residual nuclei from the even-even target  $^{28}\text{Si}$  are largest on the  $Z > N$  side of the valley of stability, while for the odd-even target  $^{27}\text{Al}$  they are largest on the  $Z < N$  side.

4. Although a large fraction of the states in the  $A = 10$  to 27 mass region is short lived, only  $\sim 10\%$  of the observed  $\gamma$  decays show Doppler broadening. This suggests that we are missing some of the weaker transitions because of broadening. Such unobserved cross sections would be largest in non-even-even nuclei where  $\gamma$  decays do not predominantly feed the first few excited states. For those  $\gamma$  transitions which show Doppler broadening, the average momentum transferred,  $\Delta p$ , is  $\sim 190$  MeV/c, similar to the results at 1.6 GeV.<sup>5</sup>

5. We found no convincing evidence for the selective population of certain residual states that was observed at 140 MeV.<sup>3,4</sup>

6. The  $2^+ \rightarrow 0^+$  transition in even-even nuclei was observed with greater intensity than would be expected if the reaction mechanism were to result primarily in a statistical population of states followed by  $\gamma$  feeding of lower states. This was also observed with 140-MeV and 1.6-GeV alphas, but it was ascribed to the phenomenon discussed in 5 (above) at 140 MeV, and it was cited as evidence

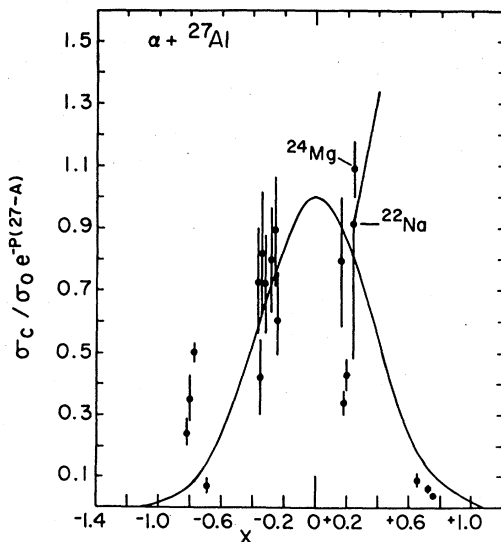


FIG. 4. Comparison of the 720-MeV  $\alpha + ^{27}\text{Al}$  cross sections (solid points) with the charge dependence of the spallation-yield formula (solid line) plotted as a function of  $X$ , where  $X \equiv Z - SA$  (see text). The measured cross sections have been compensated for  $\gamma$ -decay systematics and renormalized to remove the exponential  $A$  dependence of the spallation yields. The error bars are discussed in the text.

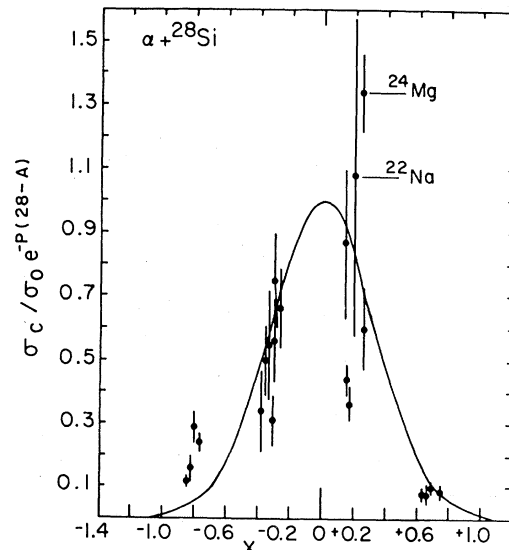


FIG. 5. Comparison of the 720-MeV  $\alpha + ^{28}\text{Si}$  cross sections (solid points) with the charge dependence of the spallation-yield formula (solid line) plotted as a function of  $X$ , where  $X \equiv Z - SA$  (see text). The measured cross sections have been compensated for  $\gamma$ -decay systematics and renormalized to remove the exponential  $A$  dependence of the spallation yields. The error bars are discussed in the text.

of a rather small average spin of the products formed after nucleon evaporation but before the  $\gamma$  cascade in the 1.6 GeV results.

7. The cross sections for production of self-conjugate residual nuclei from  $^{27}\text{Al}$  and  $^{28}\text{Si}$  showed an exponential falloff when plotted vs  $\Delta A$ . This is also true of 140-MeV  $\alpha$ 's on  $^{27}\text{Al}$  and of ~200-MeV  $\pi^{\pm}$  on  $^{27}\text{Al}$  and  $^{28}\text{Si}$ , and it suggests that a statistical mechanism is operative in these reactions.

8. When our cross sections are compensated for  $\gamma$  feeding under the assumption of a statistical initial population, they can be fitted by a spallation yield formula. For the  $^{28}\text{Si}$  target, the cross section for the self-conjugate residual nucleus  $^{24}\text{Mg}$  is considerably larger than predicted by this formula.

Thus we were able to extend the previous work on

medium-energy  $\alpha$ -induced reactions and to confirm some of the earlier conclusions. We also observed some of the expected similarities and differences between alpha- and pion-induced reactions. As in previous work on  $\alpha$ -induced reactions at intermediate energies, we were only able to obtain qualitative information concerning the reaction mechanism.

#### ACKNOWLEDGMENTS

This work was supported in part by the NSF, NASA, and the Commonwealth of Virginia. We gratefully acknowledge the help of R. T. Siegel and the SREL staff. SREL was supported by NASA, the NSF, and the Commonwealth of Virginia. The work of B. Leighty was very helpful in the early stages of the data analysis.

<sup>1</sup>B. J. Lieb, H. O. Funsten, C. E. Stronach, H. S. Plendl, and V. G. Lind, *Phys. Rev. C* **18**, 1368 (1978).

<sup>2</sup>V. G. Lind, R. E. McAdams, O. H. Otteson, W. F. Denig, C. A. Goulding, M. Greenfield, H. S. Plendl, B. J. Lieb, C. E. Stronach, P. A. M. Gram, and T. Sharma, *Phys. Rev. Lett.* **41**, 1023 (1978).

<sup>3</sup>M. D. Glascock, W. F. Hornyak, C. C. Chang, and R. J. Quickle, *Phys. Rev. C* **19**, 1577 (1979).

<sup>4</sup>W. F. Hornyak, M. D. Glascock, C. C. Chang, and J. R. Wu, *Phys. Rev. C* **19**, 1595 (1979).

<sup>5</sup>T. Shibata, H. Ejiri, J. Chiba, S. Nagamiya, K. Nakai, R. Anholt, H. Bowman, J. G. Ingersoll, E. A. Rauscher, and J. O. Rasmussen, *Nucl. Phys.* **A308**, 513 (1978).

<sup>6</sup>R. R. Doering, T. C. Schweizer, S. T. Thornton, L. C. Dennis, K. R. Cordell, K. O. H. Ziocck, and J. C. Comiso, *Phys. Rev. Lett.* **40**, 1433 (1978).

<sup>7</sup>S. T. Thornton, K. R. Cordell, L. C. Dennis, R. R. Doering, and T. C. Schweizer, *Phys. Rev. C* **19**, 913 (1979).

<sup>8</sup>T. C. Schweizer, R. R. Doering, S. T. Thornton, L. C. Dennis, K. R. Cordell, and R. L. Parks, *Phys. Rev. C* **19**, 1408 (1979).

<sup>9</sup>F. Ajzenberg-Selove, *Nucl. Phys.* **A320**, 1 (1979); **A248**, 1 (1975); **A268**, 1 (1976); **A281**, 1 (1977); **A300**, 1 (1978).

<sup>10</sup>P. M. Endt and C. Van der Leun, *Nucl. Phys.* **A310**, 1 (1978).

<sup>11</sup>C. W. Lewis, *Nucl. Instrum. Methods* **123**, 289 (1975).

<sup>12</sup>B. J. Lieb, W. F. Lankford, S. H. Dam, H. S. Plendl, H. O. Funsten, W. J. Kossler, V. G. Lind, and A. J. Buffa, *Phys. Rev. C* **14**, 1515 (1976).

<sup>13</sup>G. Rudstam, *Z. Naturforsch.* **21a**, 1027 (1966).